THE STROKE VOLUME AND THE CARDIAC OUTPUT BY THE IMPEDANCE CARDIOGRAPHY

M. C. IPATE[1], A. A. DOBRE[2], A. M. MOREGA[3]

Acest studiu este despre impedanța cardiacă, utilizată pentru determinarea volumul sanguin, pompat de vetricul stang la o singura contractie a inimii, şi a debitul cardiac. În majoritatea articolelor privind acest subiect, persoanele participante la experiment prezintă probleme cardiace. Din acest motiv au fost efectuate teste atât pe subiecți sănătoşi cât şi pe subiecți diagnosticați cu afecțiuni cardiace. Se urmăreşte compararea rezultatelor obținute pentru volumul sanguin şi pentru debitul cardiac pentru cele două categorii de persoane, prin două metode ce vor fi detaliate în lucrare. Studiul este completat de rezultate de simulare numerică pentru ICG realizate pe un domeniu de calcul obținut prin tehnici de imagistică medicală.

This study is concerned with the noninvasive impedance cardiography (ICG) as *a measure of the stroke volume and cardiac output. In many articles on this topic, people who participate in the experiments have various heart diseases and therefore we did tests on both healthy and with different cardiac disease subjects. The aim is to compare the results obtained for stroke volume and cardiac output for the two categories of persons by two methods, which will be detailed in the paper. A numerical simulation approach to ICG based on a computational domain built out of medical images completes the study.*

Keywords: impedance cardiography, cardiac output, stroke volume, numerical simulation, finite element, medical imaging

1. Introduction

Studies about the impedance cardiography were introduced more than 50 years ago as a noninvasive technique for measuring systolic time intervals and cardiac output[4] [1]. By Pickett *et al.* [2], the impedance cardiography is a simple,

[1] PhD student, Faculty of Electrical Engineering University POLITEHNICA of Bucharest, e-mail: mcorina.ipate@amotion.pub.ro,

[2] Eng., Faculty of Electrical Engineering University POLITEHNICA of Bucharest, e-mail: alin.dobre@iem.pub.ro,

[3] Prof., Faculty of Electrical Engineering University POLITEHNICA of Bucharest, e-mail: amm@iem.pub.ro

[4] the *cardiac output* is defined as the amount of blood the left ventricle ejects into the systemic circulation in one minute, measured in liters per minute [13].

noninvasive, and in the same time inexpensive method for estimating the stroke[5] volume and cardiac output based on phase changes in thorax electrical resistivity, occurring during ejection of blood into the ascending aorta.

Impedance cardiography (ICG) uses a low-amplitude, high frequency (here, 50 kHz) alternating signal to determine the impedance of the flow of electricity through the chest. With this technique, different parameters like *stroke volume* (SV) and *cardiac output* (CO) can be further derived [3]. SV echoes the volume of blood pumped by the left ventricle at each contraction, while *CO* is the total volume of blood pumped by the ventricle per minute. ICG relies Ohm's relation, which, when applied to the thorax equivalent electric circuit, may be used to relate changes in voltage and resistance to hemodynamic parameters of the cardiac function (U – voltage [V], I – current [A], and R – resistance [Ω]). Measurements were performed with BIOPAC data acquisition system.

ICG measures the heartbeat related changes of thoracic bioimpedance *via* four sensors (electrodes) placed on the neck and thorax. Basically low constant amplitude alternating electrical current (here, either 100 μA rms or 400 μA rms) is led through the thorax by a means of a set of "current" electrodes. A measure of the associated electric field in the anatomic structure is then given by the voltage drop acquired through another set of electrodes ("voltage" electrodes) conveniently placed on the thorax (Fig. 1). This output voltage may be used to define a transfer "biological" impedance $Z(t)$: the current is held constant so the output voltage is proportional to $Z(t)$. If the system does not include inductive or capacitive elements (effects), the impedance is then resistive [3].

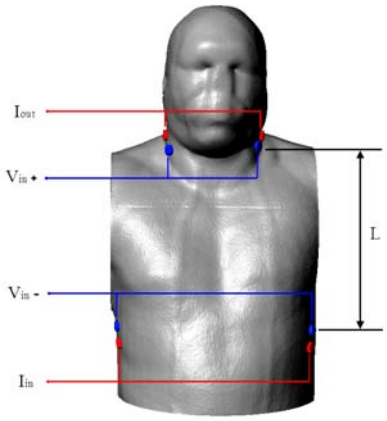

Fig. 1. Electrodes positioning used in the study [1, 2].

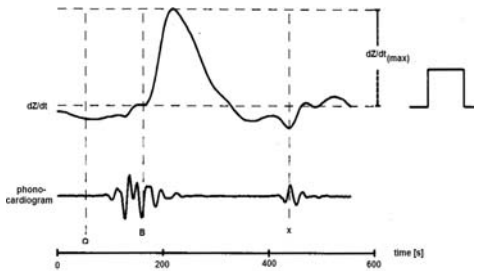

Fig. 2. dZ/dt waveform correlated with the phonocardiogram [1].

[5] the *stroke volume* is defined as the volume of blood, put out by a ventricle of the heart during a contraction cycle, measured in milliliters per beat [14].

Because blood is a good electric conductive medium when compared to the surrounding thoracic tissues, "variations in blood flow thought the great vessels result in a measurable change in impedance that allows calculation of effective SV" [4]. Changes in $Z(t)$ occurring with every heartbeat may reflect SV.

Nyboer *et al.* [5] introduced an equation relating the change in impedance (ΔZ) and base impedance (Z_0) to the volume change (ΔV) of the thorax

$$\Delta V = \rho \frac{L^2}{Z_0^2} \Delta Z, \tag{1}$$

where ρ is the electrical resistivity of blood, and L is a measure of the distance between the electrodes (and chest height).

Assuming the cylindrical model for the chest, Kubicek *et al.* [1,2] introduced a definition for SV that includes the maximum value of the time derivative of the impedance waveform $(\mathrm{d}Z/\mathrm{d}t)_{\max}$ (Fig. 2)

$$\mathrm{SV} = \rho \frac{L^2}{Z_0^2} \cdot \left(\frac{\mathrm{d}Z}{\mathrm{d}t} \right)_{\max} \cdot \mathrm{LVET}, \tag{2}$$

where LVET is the left ventricular ejection time [s], $(\mathrm{d}Z/\mathrm{d}t)_{\max}$ is the module of the maximum change rate (slope) in the impedance waveform per beat [Ω/s].

One should consider for the experiments some aspects of the parameters included in eq. (3) that could lead to errors in computed stroke volumes. It is known that $\mathrm{d}Z/\mathrm{d}t$ is prone to respiratory and movement artifacts. The interval between points *B* and *X* on the $\mathrm{d}Z/\mathrm{d}t$ waveform (Fig. 2) could not be properly measured. Sramek *et al*. [5] proposed yet another definition for SV that replaces the model used by Kubicek with a truncated cone. In this case, the size L is approximated as 17% of the patient's height (H)

$$\mathrm{SV} = \frac{(0.17H)^3}{4.2} \cdot \frac{\left(\frac{\mathrm{d}Z}{\mathrm{d}t} \right)_{\max}}{Z_0} \cdot \mathrm{LVET}. \tag{3}$$

Bernstein [5] modified eq. (4) by introducing the term δ (defined as the actual weight divided by the ideal weight), to account for deviations from ideal body weight as established by Metropolitan Life insurance tables [9]

$$SV = \delta \cdot \frac{(0.17H)^3}{4.2} \cdot \frac{\left(\frac{\mathrm{d}Z}{\mathrm{d}t} \right)_{\max}}{Z_0} \cdot \mathrm{LVET}. \tag{4}$$

Our study is concerned with SV and CO calculation using ICG measurements. Acquisition is performed with a measurement system for physiological signals, and a software package for numerical processing. We

investigated the usage of two methods for the evaluation of CO: fully computed estimates versus the processing of experimental data are the two approaches presented in the paper. The comparison between the two data sets is finally made. The main objectives are to assess SV and CO using ICG and electrocardiography signals acquisition and statistical data processing. Finally, we present an image based built volume conductor for a thorax with the aim of numerical modeling the ICG. The electric activity of the heart is neglected with respect to the ICG associated electric field.

2. Experimental Setup

The first stage, the signal acquisition, is performed following an experimental protocol applied to a group of 12 subjects, males and females, voluntarily enrolled in the program. The signal acquisition lasted for three minutes. The 12 subjects, aged between 24 and 60 years, were divided into two groups: 7 of them were considered to have normal health status (no reported cardiac problems); the other 5 were identified with different diagnosed cardiac diseases, under continuous medication.

The measurements were performed in a secluded laboratory, in a quiet atmosphere. The electrodes were positioned on the torso, in locations showed in Fig. 1 and the acquisition instruments and settings presented in [6, 7]. Electrical bioimpedance $Z(t)$, electrocardiographic signal (ECG) and heart beat rate were directly acquired using TSD 108 and DA100 BIOPAC modules [6]. Five additional on-line calculation channels were defined [8]:

- a low pass filter for the electrical bioimpedance signal, with 10 Hz cutoff frequency, and $Q = 0.707$ the quality factor[6];
- the time derivative of $Z(t)$;
- a band pass filter of heart sounds at 40-60 Hz and $Q = 0.707$;
- the absolute value of the maximum rate of change in the impedance waveform on a given beat $-\mathrm{d}Z/\mathrm{d}t$ (max);
- the heart rate (BPM), determined on the ECG channel.

The experimental protocol was implemented by using the electro-bioimpedance amplifier module EBI100C, the general purpose differential amplifier module DA100C, the physiological sounds microphone TSD 108, the electrocardiography amplifier module ECG100C, CBL 204 cables, EL 500 and EL503 electrodes. EBI100C is used to record the parameters associated with cardiac output measurements, thoracic impedance changes as a function of respiration, or any kind of biological impedance monitoring. In the same time, this module can measure the impedance and the phase. Here, the measurements are

[6] Q is defined as the measure of the sharpness of a resonant peak[15]

performed for 50 kHz, but they could also be conducted at 12.5, 25, and 100 kHz.

For heart sounds we used the physiological sounds microphone TSD108, which interfaces with the general-purpose transducer DA100C. The ECG100C amplifier is designed to pass the ECG signal with minimal distortion, with the following setup: low pass notch filter at 35 Hz – ON, high pass filter at 0.5 Hz and the gain at 1000.

EL503 module for the ECG signal recording and EBI100C are connected to EL500 (Ag-AgCl lead electrodes) electrodes, recommended for noninvasive electrophysiological signals measurements. Eight shielded electrodes (LEAD 110S) are used for the signals inputs. Ground leads are not required, since the subject is referenced via the EBI100C module.

The cardiac output (CO) was also calculated (3) for the stroke volume

$$CO = SV \cdot HR, \tag{5}$$

where HR is the heart rate (BPM) determined directly off the ECG signal.

3. Experimental Results

The analog and calculated signals are simultaneously displayed (Fig. 3). SV and CO are computed off-line. As a foresight measure, the pulse was also checked with a blood pressure electronic device.

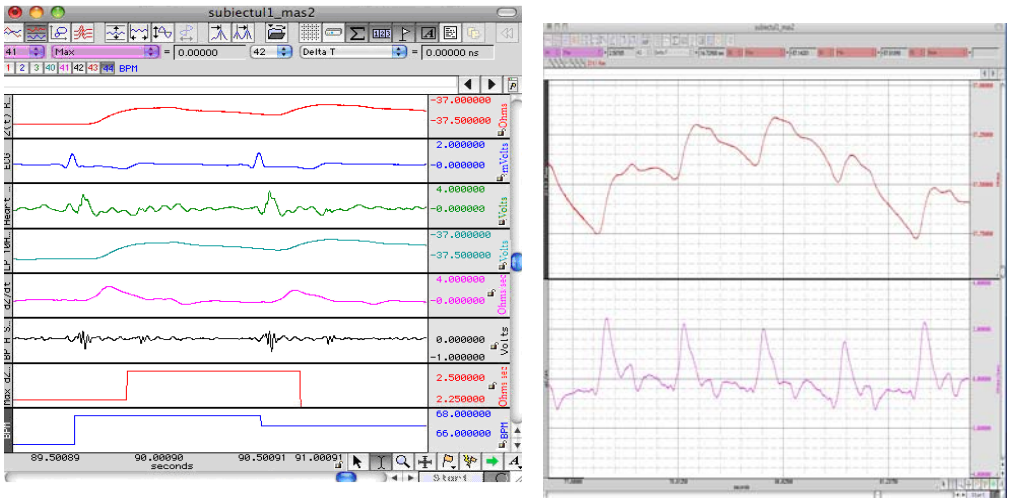

Fig. 3. Recorded and computed signals.

Table 1 shows two personalized parameters taken from the subjects: L – the distance between inner electrodes (Fig. 1) and *the left ventricular ejection*

time, LVET (or the *systolic ejection time*). *L* was measured between voltage electrodes and LVET was calculated [1], [9].

The results for one single subject (out of twelve) were considered irrelevant and eliminated; the poor placement of electrodes or the high subcutaneous fat layer led to erroneous records of $Z(t)$.

Table 1

L and LVET values

Subject	L [cm]	LVET [s]
1	31	0.291
2	30.8	0.285
3	31.2	0.294
4	32.1	0.279
5	34.7	0.288
6	32.6	0.313
7	30.6	0.282
8	37.4	0.265
9	36.3	0.277
10	36	0.293
11	35.3	0.298

The SV and CO are determined by two methods: (1) a fully computed estimate; (2) experimental data reduction. The results are finally compared.

The results obtained by the first method (fully computed estimates) are shown in Table 2. For better results or, better said, smoothed results, the settings for the cardiac output were chosen at 0.2 Hz high pass filter and a quality factor of 0.707 [6]. The mean values used in equations (3) and (6) are computed for the one minute long recording of the signals.

Table 2

SV and CO values – fully computed estimate

Subject	SV [ml/beat]	CO [liters/min]
1	57.039	3.760
2	44.778	3.330
3	73.266	5.272
4	86.927	5.393
5	64.910	5.270
6	91.508	5.582
7	69.753	5.072
8	50.716	3.984
9	54.098	3.353
10	61.931	3.742
11	59.740	4.001

SV and CO calculations in *Table 3* are exemplified by

$$\mathrm{SV} = \rho \frac{L^2}{Z_0^2} \cdot \left(\frac{dZ}{dt} \right)_{\max} \cdot \mathrm{LVET} = 127 \cdot \frac{30.6^2}{(-36.5953)^2} \cdot 2.50685 \cdot 0.282 = 62.773 \text{ ml/beat}, \quad (6)$$

$$\mathrm{CO} = \mathrm{SV} \cdot \mathrm{HR} = 62.773 \cdot 68 \cong 4.268 \text{ l/min}. \quad (7)$$

where ρ is the electrical resistivity of the blood (here, 127 Ω·cm).

Table 3

SV and CO values – experimental data reduction

Subjects	SV [ml/beat]	Pulse [BPM]	CO [liters/min]
1	60.368	67	4.044
2	41.072	80	3.285
3	68.931	73	5.031
4	73.236	75	5.492
5	58.132	94	5.464
6	82.821	74	6.128
7	62.773	68	4.268
8	41.352	81	3.349
9	58.909	54	3.181
10	59.786	67	4.005
11	60.083	68	4.085

Table 4 presents some values of the cardiac parameters (including LVET, SV and CO) synthesized from literature [1], [6].

Table 4

Cardiac output related statistics

Parameter	Value
Base thoracic impedance, Z_0 [Ω]	Males: 20–30 Females: 25–30
Change in impedance, dZ/dt [Ω/s]	0.8 – 2.5
Left-ventricular ejection time, T [s]	0.25 – 0.35
Pre-ejection time period, PEP [s]	0.05 – 0.12
Stroke volume, SV [ml/beat]	60 –100
Cardiac output, CO [l/min]	4 – 8
Cardiac index, CI [l/min/m^2] (indexed to body surface area)	2.5 – 4.5

4. A Numerical Simulation Approach to ICG

Recognizing that realistic geometries may avoid some of the errors introduced by idealizations of the computational domains, we generated a patient related image-based 3D computational model. The electrical field in the ICG problem was then solved for using the finite element method (FEM).

4.1 Image-based Computational Domain

A *Digital Imaging and Communication in Medicine* (DICOM) set of approximately 400 high resolution slices acquired from a healthy subject using a modern *Computed Tomography* (CT) scanner is the raw data used in generating the 3D computational domain [16].

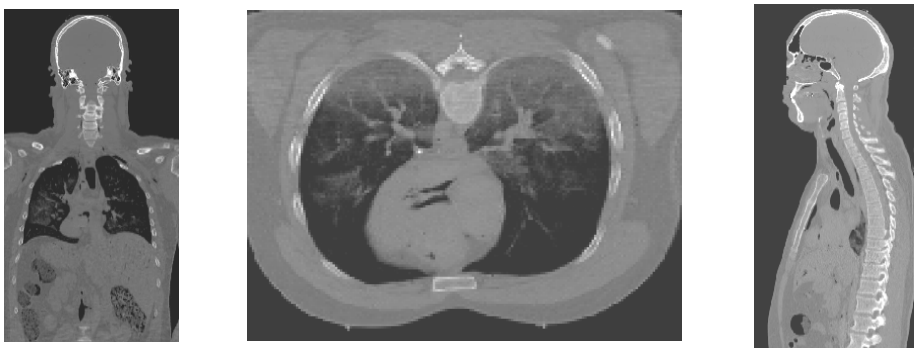

(a) (b) (c)

Fig. 5. Slices from the sagittal (a), horizontal (b) and transversal (c) workplanes.

The regions of interest (ROI) were segmented out of the image dataset source by tuning adjusting the parameters of a threshold filter [12], covering only the tissues that needed to be singled out while discarding the rest. In the end of this first and most important step of the reconstruction process, gross 3D masks of the segmented ROIs were obtained.

The 3D models were then adjusted using gaussian smoothing and binarisation filters, morphological close, erode, cavity fill and floodfill tools [12], which provided for the spatial continuity of the masks. Also, bilateral and gradient anisotropic diffusion noise filters [12] were used to remove spurious artifacts.

Fig. 6. Segmented regions of interest and mask generation.

Several subtraction, inversion and intersection boolean operations were

next applied to the segmented masks, differentiating the internal organs and tissues from the thorax and head. The ready-to-be-used version of the 3D model (Fig. 7a) is made of skull, brain, ribs, and spinal cord, miocardium, blood inside the atriums and ventricles, lungs, liver and thorax and head that embeds all these.

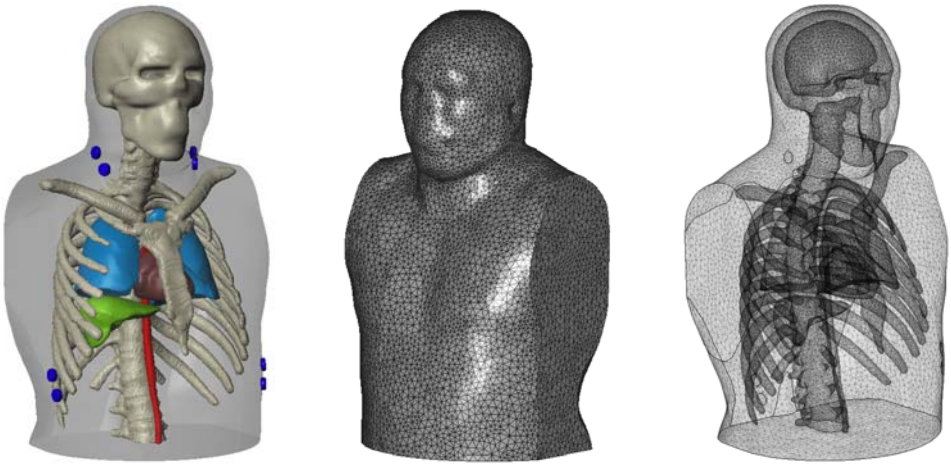

(a) (b) (c)

Fig. 7. The final 3D solid model (a) and its FEM discretization (b), (c).

The final 3D solid model was discretized, and a mesh of approximately 565,000 Lagrange tetrahedral elements was generated (Fig. 7b,c). This is the computational domain of the ICG problem.

4.2 The Mathematical Model

Consistent with the conductor volume approach to the ICG problem, the electrical field model for the signal propagation in the thoracic volume is given by: (i) the electrical charge conservation law, $\nabla \cdot \mathbf{J} = 0$; (ii) the electrical conduction law, $\mathbf{J} = \sigma \mathbf{E}$; (iii) the consequence to the electromagnetic law $\mathbf{E} = -\nabla V$.

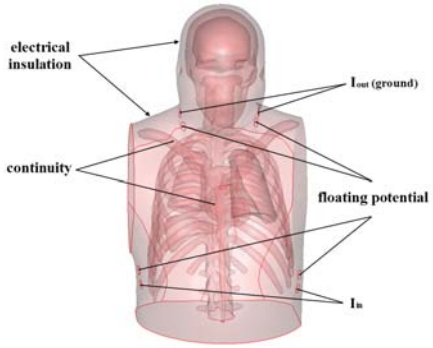

Fig. 8. The boundary conditions for the electrical field model.

Here **J** is the electrical current density [A/m^2], **E** is the electric field strength [V/m], and V is the electrical potential [V]. Summing up, the partial differential equation is

$$\Delta V = 0. \tag{9}$$

The boundary conditions (BCs) are as follows: no current inflow / outflow through the thorax surface ($\mathbf{n}\cdot\mathbf{J} = 0$). Consistent to the ICG procedure, a 100 μA electrical current is injected through the two bottom electrodes in the abdominal region, and conveyed outside the thorax through a pair of electrodes placed in the neck region. Two other pairs of electrodes provide the voltage used in calculating the *ICG* – the BC here is floating potential.

We assume that the aortic pulsatile flow is accompanied by periodic changes in the electrical conductivity of the blood, described here by the synthetic expression

$$\sigma(t) = \left[a\sin(10t) + b\right]\cdot\left[a\sin(10t - \varphi) - c\right], \tag{10}$$

where a, b, c and φ are empiric parameters used as follows: a is used to adjust the sine wave amplitude, b to shift it, c controls the cosine waveform amplitude, and φ is the cosine phase shift.

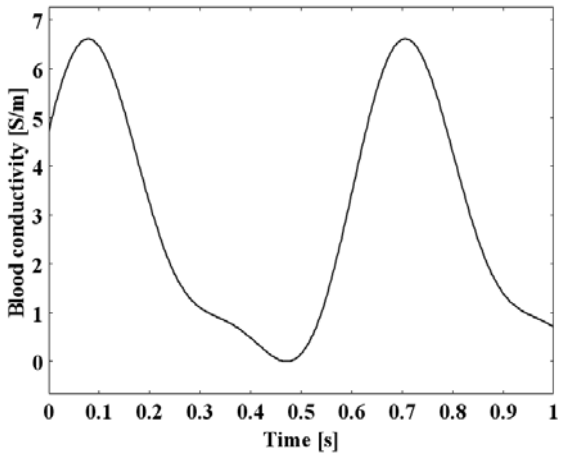

Fig. 9. The time dependent aortic blood electrical conductivity simulated by eq. (14).

The PDE (13) describing the electrical field was solved for using the finite element method (FEM) as implemented by Comsol Multiphysics, using the GMRES time dependent solver [17].

4.3 Numerical Simulation Results

A more realistic approach to the pulsatile arterial blood flow was achieved by simulating a pulse waveform to model the change in electrical conductivity of

the aortic blood, $\sigma(t)$, eq. (10). A minimum value very close to zero for the electrical conductivity of the blood is equivalent to the end of the diastolic phase, while the maximum value represents the middle of the systolic period.

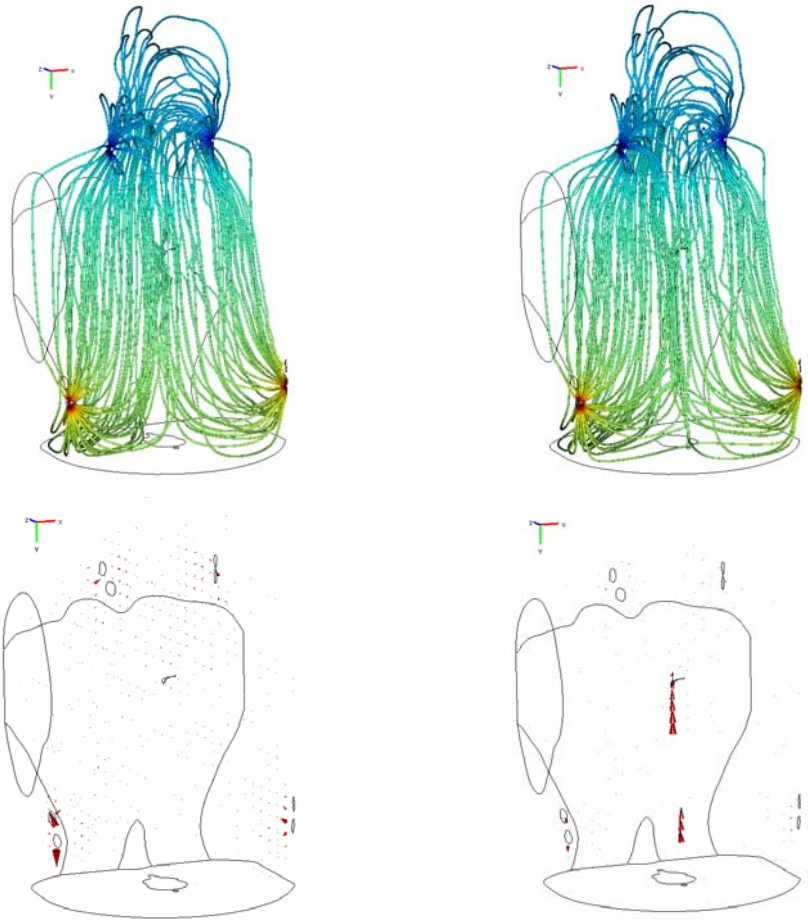

(a) (b)

Fig. 10. The electrical current density distribution in the thoracic volume for the minimum (a) and maximum (b) blood electrical conductivity values at t_{min} = 0.47 s and t_{max} = 0.705 s.

Fig. 10 shows the electrical current density for the minimum and maximum blood electrical conductivities by electrical current density lines (tubes) and arrows. At t_{max} = 0.705 s, which corresponds to the highest electrical conductivity value, the electrical current density is mainly concentrated in the aortic vessel region, while at t_{min} = 0.407 s the current density is almost evenly distributed throughout the thorax.

Due attention should be given to the boundary condition on the base surface – a cross section through the thorax. In our approach, the boundary is electrically insulated. Consequently, the electrical current cannot cross the bottom surface. A large enough computational domain, extended down to the hips, may by more appropriate to setting there the insulation BC.

The impedance values were calculated by dividing the voltage provided by be the second pairs of electrodes through the current input to the volume. The waveforms of $Z(t)$ and are presented in Fig. 11.

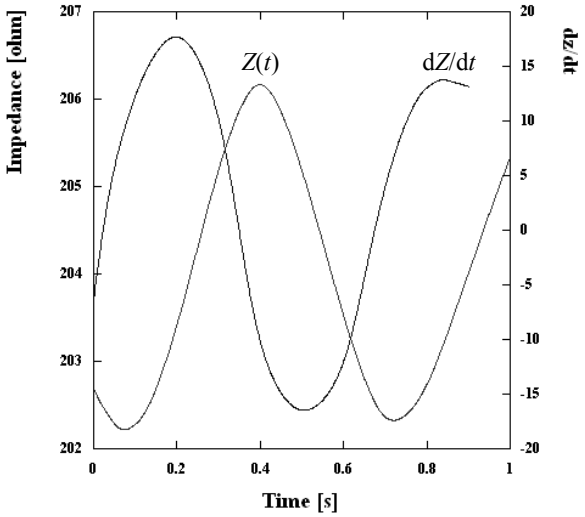

Fig. 11. The calculated impedance and its time derivative evolution.

In the near future, the electrical field model will be coupled to a hemodynamic model, in order to study the ICG problem under more realistic blood flow conditions.

5. Conclusions

From *Table 2* and *Table 3* one could observe small discrepancies between the results obtained through the two methods. The mean values for SV and CO are 65.69 ml/beat, respectively 4.45 l/min when determined with the first method (fully computed estimate), and 60.67 ml/beat and 4.39 l/min with the second method (experimental data reduction). When comparing the values in *Tables 2* and *3* with those in *Table 4* it results that, with few exceptions, they are within the limits specified there. The last four subjects are the persons with various heart diseases. They present small values for SV and CO. One person from the healthy group (subject 2) is in the same situation.

One of the causes for the small values of stroke volume, implicit of cardiac output is the less accurate positioning of electrodes. Other reason for these results is the length L, which seems to be a little higher than that from [1].

The non-invasive hemodynamic monitoring (*e.g.*, the cardiac output) most likely would decrease costs because of reduced expenditures for equipment and, why not, savings in physicians and nurses time. The information collected from this monitoring process could help avoid the potentially life-threatening complications of infection, artery perforation etc.

We aim at extending the number of persons, both the healthy and those with various diseases, and perform statistical analysis.

ICG numerical simulations were conducted on an image based realistic computational domain. The electrodes are placed on the neck and thorax. The impedance dynamics – due to the alternate filling and draining of the heart chambers and aorta with blood – was simulated by modifying the electrical conductivity. We aim to develop the ICG model for pulsatile blood flow conditions.

Acknowledgments

The work was conducted in the Laboratory for Electrical Engineering in Medicine (IEM), at UPB – a member of the BIOINGTEH platform. M.C. Ipate acknowledges the support offered by the POSDRU/6/1.5/S/19/7713 grant. A.A. Dobre acknowledges the support offered by the POSDRU/88/1.5/S/61178 grant.

R E F E R E N C E S

[1] *A. Sherwood, M.T. Allen et al*., "Committee Report: Methodological Guidelines for Impedance Cardiography", Psychophysiology, **27**, 1, 1990, U.S.A.

[2] *B. P. Pickett, J. C. Buell*, "Validity of Cardiac Output Measurement by Computer-Averaged Impedance Cardiography, and Comparison with Simultaneous Thermodilution Determinations", The American Journal of Cardiology, **69**, May 15, 1992, pp. 1354-1358.

[3] *N. M. Albert, M. D. Hail et al*., "Equivalence of the Bioimpedance and Thermodilution Methods in Measuring Cardiac Output in Hospitalized Patients with Advanced, Decompensated Chronic Heart Failure", AJCC, the American Journal of Critical Care, 2004, **13,** pp. 469-479.

[4] *S. A. Kamath, M. H. Drazner et al*.," Correlation of Impedance Cardiography with Invasive Hemodynamic Measurements in Patients with Advanced Heart Failure: the Bioimpedance CardioGraphy (BIG) Sub study of the ESCAPE Trial", Am Heart J., 2009 August, **158**, 2, pp. 217-223.

[5] *J. M. Van De Water, T. W. Miller*, "Impedance Cardiography: The next Vital Sign Technology?" Official publication of the American College of Chest Physicians, Chest 2003, **123**, pp. 2028-2033

[6] http://www.biopac.com/Manuals/app_pdf/app196.pdf

[7] http://www.biopac.com, MP System Hardware Guide, pp. 154-157.
[8] AcqKnowledge Software Guide, v.3.9, Reference Manual for AcqKnowledge® Software & MP Hardware/Firmware on Windows® XP or Mac OS® X
[9] http://btc.montana.edu/olympics/physiology/pb01.html
[10] *M. Packer, W. T. Abraham, M. R. Mehra et al.* „Utility of Impedance Cardiography for the Identification of Short- Term Risk of Clinical Decompensation in Stable Patients with Chronic Heart Failure", Journal of the American College of Cardiology, **47**, 11, 2006, pp. 2245-2252.
[11] www.biopac.com
[12] Simpleware v.3.2, Simpleware Ltd., UK, 2010.
[13] *Clyde Yancy, MD, William T. Abraham, MD*, "Noninvasive Hemodynamic Monitoring in Heart Failure: Utilization of Impedance Cardiography", Congest Heart Fail. 2004 May-Jun. **10**, 3 pp. 139.
[14] *Vedru J.,* " Electrical impedance methods for the measurement of stroke volume in man: state of art", *Acta et Comm. Univ. Tartuensis,* **974**, 1994, pp. 110-129.
[15] http://harada-sound.com/sound/handbook/process.html
[16] http://pubimage.hcuge.ch:8080/
[17] Comsol Multiphysics v3.5a, Comsol AB, Sweden, 2009.